The splitting of the electromagnon mode in conically spiral multiferroic magnets

2011 J. Phys.: Condens. Matter 23 066002

(http://iopscience.iop.org/0953-8984/23/6/066002)

J. Phys.: Condens. Matter **23** (2011) 066002 (6pp) doi:10.1088/0953-8984/23/6/066002

The splitting of the electromagnon mode in conically spiral multiferroic magnets

Hong-Bo Chen, Yi Zhou and You-Quan Li

Zhejiang Institute of Modern Physics and Department of Physics, Zhejiang University, Hangzhou 310027, People's Republic of China

Received 5 October 2010, in final form 22 November 2010
Published 24 January 2011
Online at stacks.iop.org/JPhysCM/23/066002

Abstract
In this paper, we study conically spiral multiferroic magnets with coupled magnetic and ferroelectric orders. By generalizing the spin-current model, we study spin wave excitations and electromagnons. We find that the electromagnon mode will split into two branches with different dispersions in an (external or internal) magnetic field. We apply our theory to some multiferroic materials and find that the results qualitatively agree with recent experiments. We also make predictions for new experiments.

(Some figures in this article are in colour only in the electronic version)

1. Introduction

Multiferroics are materials with both ferroelectric and magnetic orders. Multiferroics with giant magnetoelectric coupling are becoming a subject of intensive research because of their fundamental scientific importance as well as the interest that they arouse for technological applications [1–3]. This recent boom was triggered by the discovery of ferroelectricity in orthorhombically distorted perovskite manganites $RMnO_3$ (R = Tb, Dy, Gd) [4]. The spontaneous electric polarization $\vec{P}$ emerging in these multiferroics is induced by a non-trivial spin configuration, e.g. a cycloidal spiral spin ordering where spins with equal magnitudes spiral within a plane. The microscopic origin of such a magnetism-driven ferroelectricity was proposed as a spin-current mechanism [5] or an inverse Dzyaloshinskii–Moriya interaction [6, 7], and $\vec{P} \propto \vec{e}_{ij} \times (\vec{S}_i \times \vec{S}_j)$, where $\vec{e}_{ij}$ is the unit vector connecting neighboring spins at sites i and j respectively. This is the so called 'spiral mechanism' and has also been successfully applied to understand the nature of ferroelectricity in other spiral multiferroics, such as $Ni_3V_2O_8$ [8], $MnWO_4$ [9] and $LiCu_2O_2$ [10, 11].

A hallmark of magnetically induced multiferroicity is the appearance of hybridized magnon–phonon excitation which is the so called 'electromagnon' [12]. It means that a magnetic excitation can be excited by an electric field and vice versa. The first experimental evidence for such an electromagnon was recently procured through infrared optical spectroscopy measurement in $TbMnO_3$ and $GdMnO_3$ by Pimenov *et al* [13]. This pioneering work has stimulated a variety of experimental investigations concerning the low-lying collective mode in multiferroics such as perovskite $RMnO_3$ [14–23], hexagonal $YMnO_3$ [24], $BiFeO_3$ [25, 26], and RMn_2O_5 (R = Tb, Y) [27]. So far experiments have shown that electromagnons appear mainly in the spiral spin-ordered state as spontaneous electric polarization does. In most cases, the observed electromagnon behavior shows complicated magnetic modes and distinct excitation conditions. For instance, in $RMnO_3$ one can observe at least two excitation modes with energies around 2 and 8 meV. Several groups have shown that the excitation condition of the electromagnon seems to be independent of the spiral spin plane [15, 17, 19, 20]. However, a very recent report demonstrated that the excitation condition is closely associated with the spin cycloid [23]. Theoretically, Katsura *et al* [28] argued that the electromagnon observed in $RMnO_3$ at terahertz frequencies can be ascribed to the magnetoelectric coupling of the spiral mechanism, i.e. the rotation of the spiral spin plane can be excited by the electric field of light. The low-frequency electromagnon mode of optical absorption was assumed to arise from this mechanism [13, 14]. The spin-current model also predicts that the selection rule for the electromagnon should be closely associated with the spin cycloid. This prediction has been directly confirmed in a quite recent experiment by Shuvaev *et al* [23]. On the other hand, another model based on the symmetric Heisenberg exchange interaction has also been proposed [20, 29, 30]. This predicts that the high-frequency electromagnon may correspond to a zone-edge magnon and the excitation condition is tied to the structural peculiarities of distorted perovskite multiferroic manganites. Therefore, the exact nature of the electromagnon

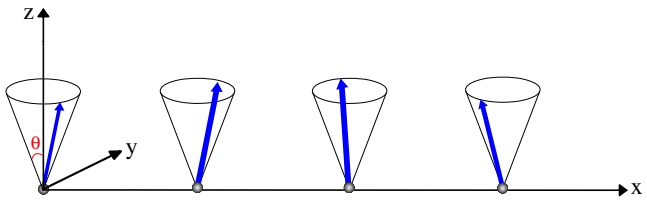

Figure 1. Conically spiral spin order in the presence of the effective Zeeman field $h_{\rm eff}$. Blue arrows denote spins which lie on the cone surface and spiral along the z-axis with a conical angle θ.

at terahertz frequencies is still a matter of debate and remains to be elucidated by further studies.

These recent results stimulated us to investigate the electromagnon so as to explore the nature of the magnetodielectric coupling in conical spiral magnets. Motivated by the fact that the induced ferroelectricity in conical multiferroics can be explained by the spin-current model proposed by Katsura *et al* [5], it is reasonable to adopt the same mechanism to investigate the low-energy collective behavior. In this paper, we extend the spin-current mechanism to conical spiral magnets and investigate the nature of the dynamical magnetoelectric coupling.

The rest of this paper is organized as follows. In section 2, we present the model and discuss the static properties of the system. In section 3, we study spin wave excitations and their dispersions. In section 4, we study electromagnons, apply our theory to some materials and compare the results with experiments. We then summarize our results in section 5.

2. Model and the multiferroic ground state

Following Katsura *et al* [28], we model an insulating multiferroic magnet as a quasi-one-dimensional spin chain along the x-direction with atomic displacement. However, in our model, spins are not in-plane but conically spiral, the cone axis is along the z-direction and the xy-plane is the helically spiral plane, as shown in figure 1. We formulate the spiral mechanism through dynamically coupled magnetic and ferroelectric order given by the following Hamiltonian:

$$H = H_1 + H_2 + H_3, \tag{1a}$$

$$H_1 = -\sum_{i,j} J_{ij}\vec{S}_i\cdot\vec{S}_j + D\sum_i (S_i^z)^2 - \gamma h_{\rm eff}\sum_i S_i^z, \tag{1b}$$

$$H_2 = -\lambda\sum_i (\vec{u}_i\times\vec{e}_x)\cdot(\vec{S}_i\times\vec{S}_{i+1}), \tag{1c}$$

$$H_3 = \sum_i\left(\frac{\kappa}{2}\vec{u}_i^2 + \frac{1}{2M}\vec{p}_i^2\right). \tag{1d}$$

The conically spiral spin order is described by H_1, where $J_{ij} = J(\vec{R}_i - \vec{R}_j)$ is the isotropic exchange coupling between $\vec{S}_i$ and $\vec{S}_j$, $\vec{R}_{i(j)}$ the spatial position of site $i(j)$, $D > 0$ is the single-ion easy-plane (xy-plane) anisotropy, γ is the gyromagnetic ratio, and $h_{\rm eff}$ is the effective Zeeman field giving rise to the out-of-plane canting. Note that $h_{\rm eff}$ may come from the intrinsic crystal field or an external magnetic field. H_2 represents the coupling between the spin degrees of freedom and the electric polarization of the ions with coupling strength λ, where $\vec{u}_i$ is the effective displacement at unit cell i and is related to a local electric dipole $e^*\vec{u}_i$ with e^* a Born charge. Notice that $\vec{u}_i$ is not the simple atomic displacement of the ion at the site i where the spin is located, e.g. Mn atoms in $RMnO_3$, but the effective displacement of the electronic cloud which may be induced by the displacement of other surrounding ions, e.g., O atoms. Therefore the $\vec{u}_i$ dependence of J is of the order of 10^{-3} [7] and can be neglected at the leading order. $\vec{u}_i$ describes phonon modes simultaneously. The dynamics of ionic polarization is given by H_3, where $\vec{p}_i$ is the canonically conjugate momentum of $\vec{u}_i$. κ and M are the stiffness and the effective mass of $\vec{u}_i$ respectively.

As proposed in [28], a plausible magnetism-driven multiferroic ground state of Hamiltonian (1*a*) in the absence of $h_{\rm eff}$ is characterized by in-plane spiral spin order coexisting with ferroelectric order. In constructing the classical ground state, equation (1*b*) is adopted firstly to determine the spin configuration $\vec{S}_i$, then equations (1*c*) and (1*d*) are used to find out the atomic displacement $\vec{u}_i$. In the presence of the effective Zeeman field $h_{\rm eff}$, the spiral spins in the xy-plane will cant toward the z-axis with a conical angle θ (see figure 1). This conically spiral order can be formulated through the spin configuration as

$$\vec{S}_i = S(\sin\theta\cos\phi_i, \sin\theta\sin\phi_i, \cos\theta), \tag{2}$$

where $\phi_i = \vec{Q}\cdot\vec{R}_i + \phi$, $\vec{Q}$ is the wavevector of the spiral order, ϕ is a phase angle, and S is the magnitude of the spin.

Minimizing the energy provided by equations (1*c*) and (1*d*) with respect to $\vec{u}_i$ leads to the ferroelectric order of the form

$$\vec{u}_i = \frac{\lambda}{\kappa}\vec{e}_x\times(\vec{S}_i\times\vec{S}_{i+1}). \tag{3}$$

Putting equation (2) into (3), we obtain

$$\vec{u}_i = -\frac{\lambda}{\kappa}S^2\sin^2\theta\sin(Qa)\,\vec{e}_y - \frac{\lambda}{\kappa}S^2\sin\theta\cos\theta(\cos\phi_i - \cos\phi_{i+1})\vec{e}_z. \tag{4}$$

Here a is the lattice constant, the x component of $\vec{u}_i$ vanishes and the y component is site-independent, while the z component changes site by site with the same wavevector $\vec{Q}$ as $\vec{S}_i$. As indicated in equation (4), there is a net atomic displacement per unit cell along the y direction $u_0^y = -\frac{\lambda}{\kappa}S^2\sin^2\theta\sin(Qa)$, resulting in a macroscopic electric polarization $\vec{P} = e^*u_0^y\vec{e}_y$, which is consistent with the experiment observations [31].

The classical ground state energy $H^{(0)}$ is given by

$$H^{(0)} = NS^2\left(-J_Q\sin^2\theta - J_0\cos^2\theta + D\cos^2\theta - \frac{\gamma h_{\rm eff}}{S}\cos\theta - \frac{1}{2}\frac{\lambda^2}{\kappa}S^2\sin^4\theta\sin^2(Qa)\right), \tag{5}$$

where N is the number of unit cells and J_q is the Fourier transform of $J(\vec{R}_i)$ with the wavevector $\vec{q}$ given by

$$J_q = \sum_i J(\vec{R}_i)\exp(\mathrm{i}\vec{q}\cdot\vec{R}_i).$$

Note that we use q instead of $\vec{q}$ because $\vec{q} = q\vec{e}_x$.

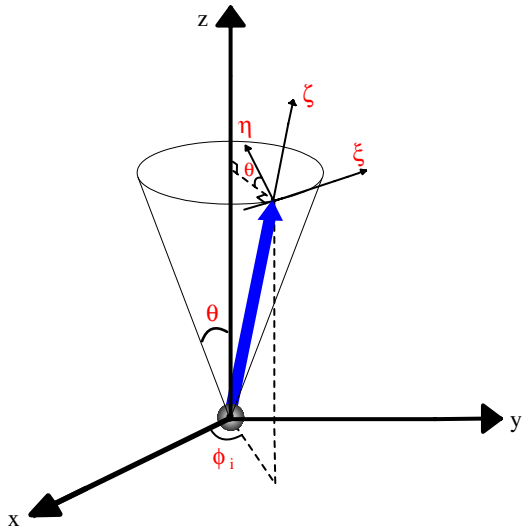

Figure 2. Local coordinates (ξ_i, η_i, ζ_i). The blue arrow denotes the local spin.

The ordering wavevector $\vec{Q}$ and conical angle θ are found at the minimum of the ground state energy $H^{(0)}$ in equation (5), i.e. $\partial H^{(0)}/\partial Q = 0$ and $\partial H^{(0)}/\partial\theta = 0$, which leads to

$$\sum_i J(\vec{R}_i)(R_i/a)\sin(QR_i) = \frac{1}{2}\frac{\lambda^2}{\kappa}S^2\sin^2\theta\sin(2Qa), \quad (6)$$

$$\cos\theta = \frac{\gamma h_{\rm eff}}{2S(J_Q - J_0 + D + \frac{\lambda^2}{\kappa}S^2\sin^2(Qa)\sin^2\theta)}. \quad (7)$$

3. Spin wave

Now we consider low-energy excitations above the multiferroic ground state discussed in section 2. We begin with spin excitations and treat the atomic displacement statically at this stage. Since spins are spirally ordered in the ground state which breaks spin rotational symmetry, gapless spin waves (magnons) will appear as Goldstone bosons naturally. Therefore we will apply spin wave theory to these spiral magnets. In contrast to conventional ferromagnets or antiferromagnets, spins spiral within a cone surface with conical angle θ. To study spin waves generalized in such a spirally ordered state, it is convenient to introduce the rotating local coordinates (ξ_i, η_i, ζ_i). The local ζ-axis is taken along the spin direction in the classical ground state, say, $\vec{e}_\zeta = \hat{S} \equiv \vec{S}/S$. The local ξ-axis is given by $\vec{e}_\xi = \frac{\vec{e}_z\times\vec{e}_\zeta}{|\vec{e}_z\times\vec{e}_\zeta|}$, which is perpendicular to the z–ζ plane. Local η is chosen to satisfy $\vec{e}_\eta = \vec{e}_\zeta \times \vec{e}_\xi$ as shown in figure 2.

It is straightforward to see the transformation between the x, y, z components of S_i and its ξ, η, ζ components [32]:

$$S_i^x = -S_i^\xi\sin\phi_i - S_i^\eta\cos\theta\cos\phi_i + S_i^\zeta\sin\theta\cos\phi_i, \quad (8a)$$

$$S_i^y = S_i^\xi\cos\phi_i - S_i^\eta\cos\theta\sin\phi_i + S_i^\zeta\sin\theta\sin\phi_i, \quad (8b)$$

$$S_i^z = S_i^\eta\sin\theta + S_i^\zeta\cos\theta. \quad (8c)$$

Then we perform Holstein–Primakoff transformation with the help of the local coordinates. The spin operators can be written in terms of boson creation and annihilation operators $a_i^\dagger$ and a_i:

$$S_i^\dagger = S_i^\xi + iS_i^\eta = \sqrt{2S}\sqrt{1 - \frac{a_i^\dagger a_i}{2S}}a_i \approx \sqrt{2S}a_i, \quad (9a)$$

$$S_i^- = S_i^\xi - iS_i^\eta = \sqrt{2S}a_i^\dagger\sqrt{1 - \frac{a_i^\dagger a_i}{2S}} \approx \sqrt{2S}a_i^\dagger, \quad (9b)$$

$$S_i^\zeta = S - a_i^\dagger a_i. \quad (9c)$$

Consequently, we can express the Hamiltonian (1*a*) as

$$H = H^{(0)} + H^{(2)},$$

with $H^{(0)}$ the ground state energy given in equation (5) and $H^{(2)}$ the noninteracting magnon Hamiltonian. The free magnon part $H^{(2)}$ reads

$$H^{(2)} = -NS[J_Q - \lambda u_0^y\sin(Qa)] + \tfrac{1}{2}\sum_q[(A(q) - B(q) - C(q))(a_q^\dagger a_q + a_q a_q^\dagger) + B(q)(a_q a_{-q} + a_q^\dagger a_{-q}^\dagger)], \quad (10a)$$

with

$$A(q) = 2S\Big[J_Q - \frac{J_{q+Q} + J_{q-Q}}{2} - \lambda u_0^y\sin(Qa)(1 - \cos(qa))\Big], \quad (10b)$$

$$B(q) = S\Big[J_q - \frac{J_{q+Q} + J_{q-Q}}{2} - D + \lambda u_0^y\sin(Qa)\cos(qa)\Big]\sin^2\theta, \quad (10c)$$

$$C(q) = 2S\Big[\frac{J_{q+Q} - J_{q-Q}}{2} - \lambda u_0^y\cos(Qa)\sin(qa)\Big]\cos\theta. \quad (10d)$$

Here $J(\vec{R}) = J(-\vec{R})$ is assumed, thus the coefficients $A(q)$ and $B(q)$ are even functions of q, while $C(q)$ is odd. Note that $C(q)$ will vanish in the absence of $h_{\rm eff}$. The quadratic term $H^{(2)}$ can be diagonalized with the help of Bogoliubov transformation,

$$\begin{aligned} a_q &= \cosh\theta_q b_q + \sinh\theta_q b_{-q}^\dagger, \\ a_{-q}^\dagger &= \cosh\theta_q b_{-q}^\dagger + \sinh\theta_q b_q, \end{aligned} \quad (11)$$

resulting in

$$H^{(2)} = -NS[J_Q - \lambda u_0^y\sin(Qa)] + \sum_q \omega_q(b_q^\dagger b_q + \tfrac{1}{2}), \quad (12)$$

with the spin wave dispersion

$$\omega_q = \sqrt{A(q)(A(q) - 2B(q))} - C(q). \quad (13)$$

Comparing with in-plane spiral order, we find that ω_q is not an even function of q in the presence of $h_{\rm eff}$, since $C(q)$ is asymmetric of q. The spin wave excitation at $q = 0$ is gapless and remains as Goldstone mode corresponding to global rotations of spins around the z axis. However, the double degeneracy of gapped modes at $q = \pm Q$ is lifted due to the $C(q)$ term. One can see in the following discussion that such an asymmetric property of the spin fluctuations with the wave vector $q = \pm Q$ is important in connection with the magnetoelectric excitations (i.e. electromagnon).

4. Electromagnon

We now further consider the collective modes by including the dynamical coupling between magnons and phonons. The hybridized spin excitations with electron polarizations, called electromagnons, are expected as new collective modes instead of magnons. To study these collective modes, we shall adopt the equations of motion and take account of only small fluctuations around the classical ground state where S_i^ζ and u_i^y are constants. Thus for spin degrees of freedom, we only invoke S_i^ξ and S_i^η as dynamical parts. From equation (1*c*), we find that only the transverse phonon modes u_i^y and u_i^z couple to spin degrees of freedom. Therefore S_i^ξ, S_i^η and u_i^z are sufficiently small dynamical quantities to represent electromagnons at the leading order.

To the linear order of S_i^ξ, S_i^η and u_i^z, the equations of motion in q-space read

$$\dot{S}_q^\eta = -A(q)S_q^\xi + \mathrm{i}C(q)S_q^\eta + \lambda S^2\cos\theta \times \left(\frac{1-\mathrm{e}^{-\mathrm{i}(q-Q)a}}{2i}\mathrm{e}^{\mathrm{i}\phi}u_{q-Q}^z - \begin{pmatrix} Q\to -Q \\ \phi\to -\phi\end{pmatrix}\right), \tag{14a}$$

$$\dot{S}_q^\xi = K(q)S_q^\eta + \mathrm{i}C(q)S_q^\xi - \lambda S^2 \times \left[\left(\frac{\mathrm{e}^{\mathrm{i}Qa}-\mathrm{e}^{-\mathrm{i}qa}}{2}\sin^2\theta + \frac{1-\mathrm{e}^{-\mathrm{i}(q-Q)a}}{2}\cos^2\theta\right) \times \mathrm{e}^{\mathrm{i}\phi}u_{q-Q}^z + \begin{pmatrix} Q\to -Q \\ \phi\to -\phi\end{pmatrix}\right], \tag{14b}$$

$$\dot{u}_q^z = \frac{1}{M}p_q^z, \tag{14c}$$

$$\dot{p}_q^z = -\kappa u_q^z + \lambda S \times \left[\frac{(\mathrm{e}^{\mathrm{i}Qa}-\mathrm{e}^{\mathrm{i}(q-Q)a})\sin^2\theta + (1-\mathrm{e}^{\mathrm{i}qa})\cos^2\theta}{2} \times \mathrm{e}^{\mathrm{i}\phi}S_{q-Q}^\eta + \begin{pmatrix} Q\to -Q \\ \phi\to -\phi\end{pmatrix}\right] + \lambda S\left[\cos\theta\frac{1-\mathrm{e}^{\mathrm{i}qa}}{2\mathrm{i}}(\mathrm{e}^{\mathrm{i}\phi}S_{q-Q}^\xi - \mathrm{e}^{-\mathrm{i}\phi}S_{q+Q}^\xi) + S\sin\theta\cos\theta\left(\frac{\mathrm{e}^{\mathrm{i}Qa}-1}{2}\delta_{q,Q}\mathrm{e}^{\mathrm{i}\phi} + \frac{\mathrm{e}^{-\mathrm{i}Qa}-1}{2}\delta_{q,-Q}\mathrm{e}^{-\mathrm{i}\phi}\right)\right], \tag{14d}$$

with

$$K(q) = A(q) - 2B(q), \tag{15}$$

where $A(q)$, $B(q)$ and $C(q)$ are given in equations (10). When $\lambda = 0$, the spin waves are decoupled from phonon modes, and we can derive the spin wave dispersion in equation (13) from equations (14*a*) and (14*b*). For $\lambda \neq 0$, in analogy to the cycloidally spiral spin state, spins and electric polarizations couple to each other in the conically spiral spin state. S^ξ and S^η together give rise to spin wave modes as in equation (13). From equations (14), one sees that the spin wave at q is coupled to the phonon mode $u_{q\pm Q}$ and, conversely, u_q is coupled to $S_{q\pm Q}^{\xi(\eta)}$. When the conical angle $\theta = \pi/2$, the conically spiral state becomes a cycloidally spiral state and equations (14) will coincide with those obtained by Katsura *et al* [28].

Now we shall investigate ac dielectric properties and electromagnon modes. For these purposes, we utilize the retarded Green's function $G^\mathrm{R}(AB; t-t')$ defined by

$$G^\mathrm{R}(AB; t-t') = -\mathrm{i}\theta(t-t')\langle[A(t), B(t')]\rangle, \tag{16}$$

and its frequency representation

$$G^\mathrm{R}(AB;\omega) = \frac{1}{2\pi}\int_{-\infty}^{\infty} G^\mathrm{R}(AB;t)\mathrm{e}^{\mathrm{i}\omega t}, \tag{17}$$

where $A, B = u_q^z, p_q^z, S_q^\xi, S_q^\eta$. These Green's functions can be determined from a set of generic equations of motion whose Fourier transform is

$$\omega\langle\langle A; B\rangle\rangle_\omega = \frac{1}{2\pi}\langle[A, B]\rangle + \langle\langle[A, H]; B\rangle\rangle_\omega. \tag{18}$$

Here we denote $G^\mathrm{R}(AB;\omega) = \langle\langle A; B\rangle\rangle_\omega$. The dielectric function $\varepsilon_{zz}(\omega)$ can be obtained from the Green's function through $\varepsilon_{zz}(\omega) = 1 - 4\pi(e^*)^2 G^\mathrm{R}(u_{q=0}^z u_{q=0}^z;\omega)$. The frequency dispersions of electromagnons are given by the poles of the Green's functions, e.g., $G^\mathrm{R}(u_q^z u_{-q}^z;\omega)$.

In particular, we are interested in phonon modes near $q = 0$ (associated with magnon modes near $q = \pm Q$) which can be typically probed by optical experiments. With the help of equations (14) and (18), one easily derives the displacement Green's function

$$\langle\langle u_0^z; u_0^z\rangle\rangle = \frac{1}{2\pi M}\{(\omega^2-\omega_Q^2)(\omega^2-\omega_{-Q}^2)\}\Big\{(\omega^2-\omega_0^2) \times (\omega^2-\omega_Q^2)(\omega^2-\omega_{-Q}^2) - \frac{2\lambda^2 S^3\sin^2(Qa)\sin^4\theta}{\kappa} \times A(Q)\omega_0^2(\omega^2-\omega_Q\omega_{-Q})\Big\}^{-1}, \tag{19}$$

where $\omega_{\pm Q}$ is given by equation (13) and $\omega_0 = \sqrt{\kappa/M}$ is the frequency of the original phonon. Note that in deriving equation (19), we only keep the components at $q = 0$ and $q = Q$ and neglect others. There are three pairs of poles, $\pm\omega_{1,2,3}$, at the real axis in the complex ω plane in the dynamical dielectric function $\langle\langle u_0^z; u_0^z\rangle\rangle$. Note that when $\theta = \pi/2$, $\omega_{-Q} = \omega_Q$, the pairs of poles in $\langle\langle u_0^z; u_0^z\rangle\rangle$ will reduce to two. That is what is observed in the experiments on $TbMnO_3$ and $GdMnO_3$ [13] and explained in the framework of the cycloidally spiral mechanism [28].

As estimated for realistic material later, when $D, J \ll \kappa a^2$ and $\lambda \ll \kappa a$, we have $\omega_{\pm Q} \ll \omega_0$ and can approximately obtain the three frequencies of hybridized phonon modes as follows: $\omega_1 \approx \omega_0$, $\omega_2 \approx \omega_Q$, $\omega_3 \approx \omega_{-Q}$. As long as $\theta < \pi/2$, the spiral order is not cycloidal but conical, the two lower frequencies $\omega_2 \neq \omega_3$, say, there occurs splitting of electromagnon modes.

Now we shall proceed with a rough estimate of the splitting $\Delta\omega \equiv \omega_3 - \omega_2$ and a comparison with experimental observations in $RMnO_3$ in the presence of an external magnetic field perpendicular to the cycloidal plane [16, 21]. Typically, the superexchange $J \sim 0.8$ meV and the single-ion anisotropy $D \sim 0.4$ meV for perovskite manganites $RMnO_3$ [22]. The spin–lattice coupling is estimated as $\lambda \sim 1$ meV Å^{-1} and

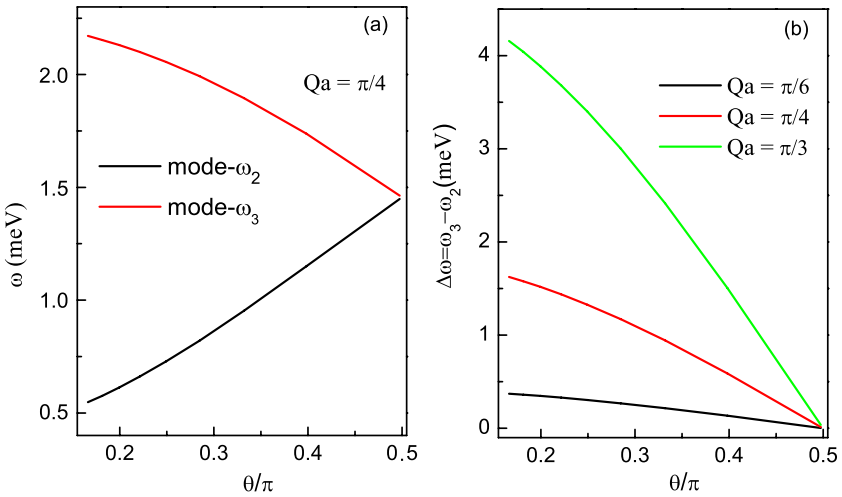

Figure 3. Behavior of electromagnon splitting in transverse conical magnets. (a) The two electromagnon modes ω_2 and ω_3 as a function of canting angle θ for $Qa = \pi/4$. (b) Electromagnon difference $\Delta\omega = \omega_3 - \omega_2$ versus the canting angle θ for the cases $Qa = \pi/6, \pi/4$ and $\pi/3$.

the stiffness $\kappa \sim 1$ eV Å^{-2} [7]. The lattice constant $a \sim 1$ Å. Thus the conditions $D, J \ll \kappa a^2$ and $\lambda \ll \kappa a$ are satisfied, and we have $\omega_{\pm Q} \ll \omega_0$, $\omega_2 \approx \omega_Q$, $\omega_3 \approx \omega_{-Q}$ in the multiferroic magnet $TbMnO_3$. Thus $\Delta\omega = 2C(Q) \sim JS\cos\theta$. Then we estimate the conical angle θ and thereby $\cos\theta$ from equation (7). Since $\lambda/(\kappa a) \sim 10^{-3}$, we simply have $\cos\theta \sim \gamma h_{\rm eff}/(2JS)$. Thus $\Delta\omega \sim \gamma h_{\rm eff}/2$, where $\gamma = g\mu_{\rm B}$ and the Landé g factor $g \sim 1$ is assumed. Experimentally, an external magnetic field is applied perpendicularly to the cycloidal plane up to 7 T [16, 21], therefore we have $\Delta\omega \sim 1$ meV.

The dependence of the two collective modes ω_2 and ω_3 on the canting angle θ is shown in figure 3(a) with $Qa = \pi/4$. We adopt $S = 2$ here since the spins come from $Mn^{3+}(3d^4)$ ions. One sees that the splitting of the electromagnon $\Delta\omega$ decreases when the canting angle θ increases, in other words, it increases with the magnetic field increase. The two modes merge at $\theta = \pi/2$ and the splitting vanishes, which is the in-plane cycloidal limit discussed by Katsura *et al* [28]. Another observation is that ω_3 and ω_2 are higher and lower than the cycloidal spiral ones, respectively. The splitting of the electromagnon under an external magnetic field has indeed been observed by Pimenov *et al* in $Eu_{1-x}Y_xMnO_3$ [16] and $TbMnO_3$ [21] when the external magnetic field is applied perpendicularly to the cycloidal spin plane. For the special case of $x = 0.2$ for $Eu_{1-x}Y_xMnO_3$, an electromagnon mode can be clearly observed with frequency close to 24 cm^{-1}. However, this mode splits into two electromagnons under the external magnetic field. The splitting of the electromagnon increases with the increase of magnetic field, which is similar to our calculation as shown in figure 3(a). Since Pimenov *et al* argued that the ferroelectric ground state is a weak conical-like spiral order, the splitting of the electromagnon under the magnetic field may be ascribed to the conical spiral order according to our observation. Very recently, the splitting of electromagnons has been also observed in $TbMnO_3$ [21] with a perpendicular magnetic field applied along the a-axis. Instead of the initial two electromagnons, four new modes have been observed in the spectra. Pimenov *et al* argued that these distinct characteristics of the electromagnon may be attributed to the complexity of the tilted spin cycloid due to the perpendicularly applied magnetic field. Experimentally, the magnitude of the applied magnetic field is about 7 T in $TbMnO_3$. From equation (7) we can estimate $\cos\theta \cong 0.4$ and thereby $\Delta\omega \sim 0.8$ meV. Our calculation coincides with experimental results qualitatively. The canting angle dependence of $\Delta\omega$ is also shown in figure 3(b), for $Qa = \pi/6, \pi/4, \pi/3$. It is shown that the splitting increases with Qa.

Another interesting compound is spinel cobalt chromite $CoCr_2O_4$. Being a very rare example of a single-phase multiferroic material, it has received much interest from the viewpoint of multiferroicity [31, 33–37]. Below $T_S = 26$ K, spontaneous electric polarization appears and the magnetic ions (Co^{2+} and Cr^{3+}) develop a conically spiral spin order. The conical angle θ is 48° for Co^{2+} and 71° for Cr^{3+} respectively [31]. The static and dynamical properties of the conical spiral magnets have been studied based on Ginzburg–Landau theory [38, 39]. A spin model was also proposed to give rise to the conically spiral ordered state [40]. We now apply our theory to this compound by assuming previous parameters, such as J, D, etc. We expect that $\Delta\omega \sim 0.9$ meV and 0.5 meV will be observed for Co^{2+} and Cr^{3+} respectively.

There exist many other interesting multiferroic compounds with magnetic field induced conically spiral spin order, such as $Eu_{0.55}Y_{0.45}MnO_3$ [41], proper screw-type helimagnet $ZnCr_2Se_4$ [42, 43], Y-type hexaferrite $Ba_2Mg_2Fe_{12}O_{22}$ [44, 45]. Our theory will be applicable when spiral spin orders exist. Note that ω_2 and ω_3 depend on the canting angle θ which is tunable through the external field. This provides a possibility to manipulate electromagnons.

5. Summary

We have studied conically spiral multiferroic magnets by generalizing the spin-current model. We have shown that a conically spiral multiferroic shows unique dynamical

magnetoelectric properties which are different from a conventional cycloidal magnet. We found that the magnon mode at $q = 0$ remains gapless and the doubly degenerate gapful modes at $q = \pm Q$ are lifted. The hybridized collective excitation—the electromagnon—splits into two branches, in contrast to the in-plane cycloidal spiral situation where only one electromagnon dispersion is observed. The theoretical results agree with existing experiments well and we make predictions for other compounds.

We expect that our theoretical investigations will provide a clue for experimentalists to elucidate the novel multiferroic excitations in external or internal (effective) magnetic field induced conically spiral multiferroic materials.

Acknowledgments

This work is supported by NSFC (Grant Nos 11074216, 10874149 and 11074218), National Basic Research Program of China (973 Program, No. 2011CBA00103), and the Fundamental Research Funds for the Central Universities in China.

References

[1] Cheong S-W and Mostovoy M 2007 *Nat. Mater.* **6** 13
[2] Loidl A, von Loehneysen H and Kalvius G M (ed) 2008 *J. Phys.: Condens. Matter* **20** 430301 (special issue)
[3] Khomskii D 2009 *Physics* **2** 20
[4] Kimura T, Goto T, Shintani H, Ishizaka K, Arima T and Tokura Y 2003 *Nature* **426** 55
[5] Katsura H, Nagaosa N and Balatsky A V 2005 *Phys. Rev. Lett.* **95** 057205
[6] Mostovoy M 2006 *Phys. Rev. Lett.* **96** 067601
[7] Sergienko I A and Dagotto E 2006 *Phys. Rev.* B **73** 094434
[8] Lawes G *et al* 2005 *Phys. Rev. Lett.* **95** 087205
[9] Taniguchi K, Abe N, Takenobu T, Iwasa Y and Arima T 2006 *Phys. Rev. Lett.* **97** 097203
[10] Park S, Choi Y J, Zhang C L and Cheong S-W 2007 *Phys. Rev. Lett.* **98** 057601
[11] Seki S, Yamasaki Y, Soda M, Matsuura M, Hirota K and Tokura Y 2008 *Phys. Rev. Lett.* **100** 127201
[12] Bar'yakhtar V G and Chupis I E 1970 *Sov. Phys.—Solid State* **11** 2628
[13] Pimenov A, Mukhin A A, Ivanov V Y, Travkin V D, Balbashov A M and Loidl A 2006 *Nat. Phys.* **2** 97
[14] Senff D, Link P, Hradil K, Hiess A, Regnault L P, Sidis Y, Aliouane N, Argyriou D N and Braden M 2007 *Phys. Rev. Lett.* **98** 137206
[15] Aguilar R V, Sushkov A B, Zhang C L, Choi Y J, Cheong S-W and Drew H D 2007 *Phys. Rev.* B **76** 060404
[16] Pimenov A, Loidl A, Mukhin A A, Travkin V D, Ivanov V Yu and Balbashov A M 2008 *Phys. Rev.* B **77** 014438
[17] Kida N, Ikebe Y, Takahashi Y, He J P, Kaneko Y, Yamasaki Y, Shimano R, Arima T, Nagaosa N and Tokura Y 2008 *Phys. Rev.* B **78** 104414
[18] Takahashi Y, Kida N, Yamasaki Y, Fujioka J, Arima T, Shimano R, Miyahara S, Mochizuki M, Furukawa N and Tokura Y 2008 *Phys. Rev. Lett.* **101** 187201
[19] Kida N, Yamasaki Y, Shimano R, Arima T and Tokura Y 2008 *J. Phys. Soc. Japan* **77** 123704
[20] Aguilar R V, Mostovoy M, Sushkov A B, Zhang C L, Choi Y J, Cheong S-W and Drew H D 2009 *Phys. Rev. Lett.* **102** 047203
[21] Pimenov A, Shuvaev A, Loidl A, Schrettle F, Mukhin A A, Travkin V D, Ivanov V Yu and Balbashov A M 2009 *Phys. Rev. Lett.* **102** 107203
[22] Lee J S, Kida N, Miyahara S, Takahashi Y, Yamasaki Y, Shimano R, Furukawa N and Tokura Y 2009 *Phys. Rev.* B **79** 180403
[23] Shuvaev A M, Travkin V D, Ivanov V Yu, Mukhin A A and Pimenov A 2010 *Phys. Rev. Lett.* **104** 097202
[24] Pailhès S, Fabrèges X, Règnault L P, Pinsard-Godart L, Mirebeau I, Moussa F, Hennion M and Petit S 2009 *Phys. Rev.* B **79** 134409
[25] Cazayous M, Gallais Y, Sacuto A, de Sousa R, Lebeugle D and Colson D 2008 *Phys. Rev. Lett.* **101** 037601
[26] Rovillain P, Cazayous M, Gallais Y, Sacuto A, Lobo R P S M, Lebeugle D and Colson D 2009 *Phys. Rev.* B **79** 180411(R)
[27] Sushkov A B, Aguilar R V, Park S, Cheong S-W and Drew H D 2007 *Phys. Rev. Lett.* **98** 027202
[28] Katsura H, Balatsky A V and Nagaosa N 2007 *Phys. Rev. Lett.* **98** 027203
[29] Miyahara S and Furukawa N 2008 arXiv:0811.4082
[30] Stenberg M P V and de Sousa R 2009 *Phys. Rev.* B **80** 094419
[31] Yamasaki Y, Miyasaka S, Kaneko Y, He J-P, Arima T and Tokura Y 2006 *Phys. Rev. Lett.* **96** 207204
[32] Nagamiya T 1967 *Solid State Physics* vol 20, ed F Seitz, D Turnbull and H Ehrenreich (New York: Academic) p 305
[33] Lawes G, Melot B, Page K, Ederer C, Hayward M A, Proffen Th and Seshadri R 2006 *Phys. Rev.* B **74** 024413
[34] Kim I, Oh Y S, Liu Y, Chun S H, Lee J-S, Ko K-T, Park J-H, Chung J-H and Kim K H 2009 *Appl. Phys. Lett.* **94** 042505
[35] Choi Y J, Okamoto J, Huang D J, Chao K S, Lin H J, Chen C T, van Veenendaal M, Kaplan T A and Cheong S-W 2009 *Phys. Rev. Lett.* **102** 067601
[36] Yao X, Lo V C and Liu J-M 2009 *J. Appl. Phys.* **106** 073901
[37] Chang L J, Huang D J, Li W-H, Cheong S-W, Ratcliff W and Lynn J W 2009 *J. Phys.: Condens. Matter* **21** 456008
[38] Zhang C, Tewari S, Toner J and Das Sarma S 2008 *Phys. Rev.* B **78** 144426
[39] Tewari S, Zhang C, Toner J and Das Sarma S 2008 *Phys. Rev.* B **78** 144427
[40] Scaramucci A, Kaplan T A and Mostovoy M 2009 arXiv:0906.5298
[41] Murakawa H, Onose Y, Kagawa F, Ishiwata S, Kaneko Y and Tokura Y 2008 *Phys. Rev. Lett.* **101** 197207
[42] Siratori K and Kita E 1980 *J. Phys. Soc. Japan* **48** 1443
[43] Murakawa H, Onose Y, Ohgushi K, Ishiwata S and Tokura Y 2008 *J. Phys. Soc. Japan* **77** 043709
[44] Ishiwata S, Taguchi Y, Murakawa H, Onose Y and Tokura Y 2008 *Science* **319** 1643
[45] Ishiwata S, Taguchi Y, Tokunaga Y, Murakawa H, Onose Y and Tokura Y 2009 *Phys. Rev.* B **79** 180408(R)